J Mater Sci (2007) 42:588–594
DOI 10.1007/s10853-006-0832-y

Formability of continuous cast 5052 alloy thin sheets

Hanliang Zhu · A. K. Ghosh · K. Maruyama

Received: 16 December 2004 / Accepted: 21 November 2005 / Published online: 24 December 2006

Abstract The formability of continuous cast 5052 alloy thin sheets from two different process schedules was examined. One was prepared in the laboratory by cold-rolling from a continuous cast thick plate followed by annealing (lab-processed sheet), and the other was produced by a new process involving hot-rolling followed immediately by in-line annealing (in-line annealed sheet). Tensile test results indicate that all the lab-processed sheets exhibit evident yield behavior. Increasing rolling reduction results in an increase of strength and a decrease of ductility in the lab-processed sheets due to increasing contribution of centerline segregation of second-phase particles. Both the lab-processed sheets annealed at 400 °C for 90 min and the in-line annealed sheets exhibit tensile elongation of more than 20% and two-stage strain hardening behavior. Compared with the lab-processed sheets, the in-line annealed sheet annealed at 454 °C has higher values of UTS and elongation. Furthermore, forming limit curves were determined. It is found that the level of the forming limit curve of the lab-processed thin sheet is lower than that of conventionally produced 5052-O Al, but close to that of 6111-T4 Al sheet. Moreover, the in-line annealed sheets have higher limit strains than the lab-processed sheets. These results demonstrate that the in-line annealing process results in the production of continuous cast alloy sheet with improved formability.

H. Zhu (✉) · K. Maruyama
Graduate School of Environmental Studies, Tohoku University, 02 Aobayama, Aobaku, Sendai 980-8579, Japan
e-mail: hlzhu32@yahoo.com

A. K. Ghosh
Department of Materials Science and Engineering, University of Michigan, Ann Arbor, MI 48109, USA

Introduction

The conventional production of aluminum sheet and plate products by ingot metallurgy and rolling processes involves multiple steps of hot- and cold-rolling and annealing of large ingots [1]. In contrast, the production of aluminum sheets, starting from continuous cast slab, includes only hot-rolling, cold-rolling and an optional final annealing [1]. Therefore, thin sheets produced by continuous casting may have economic advantage over conventionally produced thin sheets due to shortening of the production chain and period [2–4]. Furthermore, a new process involving hot-rolling followed immediately by in-line annealing was developed for continuous cast alloy sheet recently. This process has been expected to result in the production of continuous cast alloy sheet with improved formability at high levels of productivity, consistency and quality. However, very limited work on the mechanical property and formability of the continuous cast alloy sheet has been carried out, particularly its forming limit behavior under biaxial stretching condition.

A useful parameter for evaluation of biaxial forming capabilities is forming limit curves used for determining the formability in sheet metal stamping process. The forming limit curve defines the maximum strain before the onset of a neck or a tear in the sheet and is

expressed in terms of maximum tensile strain as a function of minor strain in the sheet surface [5–7]. The forming limit curves have proved very useful in diagnosing actual and potential problems in sheet forming [8], and have been widely applied to evaluate the formability of various aluminum and steel sheets [7, 9–11].

In this study, the mechanical properties and forming limit curves of continuous cast 5052 alloy sheets were evaluated and compared with data of conventionally produced aluminum sheets. The thin sheets were prepared from two different process schedules. One was fabricated by cold-rolling using several rolling passes from a 3.2 mm thick plate received from continuous cast and hot-rolled condition, and then the cold-rolled sheets were annealed prior to tests. This sheet is referred to as the lab-processed sheet. The other was produced by the developed process involving continuous casting and hot-rolling followed immediately by in-line annealing, and this sheet is noted as the in-line annealed sheet in this paper. The microstructures of the lab-processed sheets were examined to illustrate the effect of cold-rolling on the mechanical property and formability.

Experimental procedure

To produce thin sheets (lab-processed sheet), the continuous cast 5052 plate with thickness of 3.2 mm was first cold-rolled to sheets with two different thickness: 0.8 and 1.6 mm. Then, to determine the appropriate annealing condition for the O temper, the cold-rolled sheet with thickness of 0.8 mm was annealed at 350, 400 and 450 °C for 90 min, respectively, and air-cooled. All the cold-rolled sheets for tensile tests and punch tests were annealed at this appropriate annealing condition. The in-line annealed sheet with thickness of 2.0 mm was produced by hot-rolling process followed immediately by in-line annealing. To determine the optimum annealing condition, the in-line annealing temperatures were selected as 343, 371, 413 and 454°C.

Tensile specimens of size ASTM E8 (*g.l.* = 50.8 mm) were cut from the lab-processed sheets and the in-line annealed sheets. All tensile tests were performed on a 5505 Instron testing machine with crosshead velocity of 1 mm/min and an extensometer of size 50.8 mm. For microstructural examination, the lab-processed sheet specimens were aged at 160 °C for 15 h to cause precipitation to decorate the grain boundaries, and then polished and etched in the Keller's reagent. The grain length and thickness were determined by a linear intercept method.

To construct forming limit curve, four rectangular sheet specimens were deformed over a hemispherical punch. Specimen widths and lubrication were varied to obtain different strain paths. Two specimens were the same width (127 × 127 mm), and the other two specimens were 127 × 114 mm and 127 × 51 mm, respectively. To measure and calculate the principal strains, all specimens were electrochemically etched with circle grids of diameter of 2.54 mm. The punch tests were conducted by using dry (no lube) sheets on three of the samples, and using rubber and oil between punch and specimen for one of the 127 × 127 mm size sample. The punch tests were conducted on an apparatus, which was mounted on an Instron-1116 testing machine with 250 kN capacity. The diameters of the hemispherical steel punch and the circular die opening are 101.6 and 110.1 mm, respectively. The sheet was firmly clamped between the die plate using blank holding pressure, and the punch was moved to press against the sheet causing it plastically deform until it failed. The displacement rate of punch was kept constant at 0.02 mm/s and the punch load was monitored in order to stop the test at the point of necking or a small crack (indicated by load drop).

After punch tests, the deformed circles in the vicinity of failure were read by precision digital microscopy method. First, the deformed circles were replicated on flat paper. Then, they were photographed by digital camera connected to a computer. The deformed circle sizes (along the major and minor axes) were measured from the digital picture. At last, the major strain and minor strain were calculated and plotted to construct a forming limit curve.

Results and discussion

Microstructure of the lab-processed sheet

The microstructures of sheet cross-sections containing the thickness direction and the rolling direction of specimens with thickness of 0.8 and 1.6 mm, from the center region and the near-surface region of specimens are shown in Figs. 1 and 2. The grains are severely elongated along the rolling direction for all the specimens, which characterizes typical deformation grain structures of aluminum alloys [1]. Two kinds of second-phase particles are dispersed in the Al matrix. The fine particles were precipitated during the aging treatment and the coarse ones were initially formed during

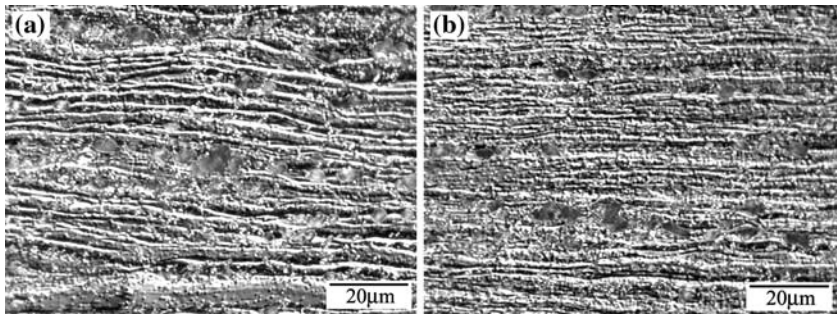

Fig. 1 Microstructure in the thickness direction of the lab-processed sheet with thickness of 0.8 mm, annealed at 400 °C for 90 min and aged at 160 °C for 15 h. (**a**) Microstructure in the center region, (d_l = 13 μm, d_t = 1.8 μm), (**b**) microstructure in the near-surface region (d_l = 10 μm, d_t = 1.3 μm)

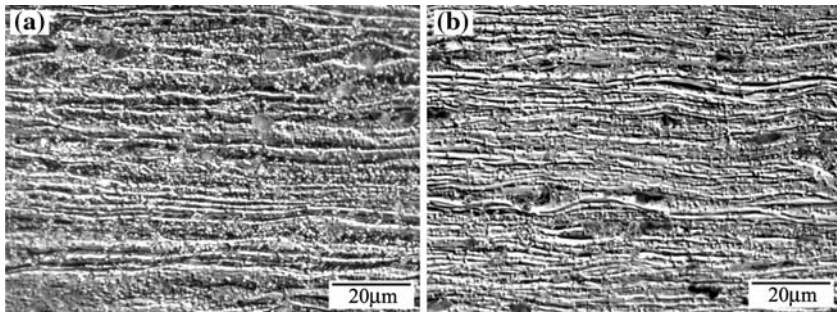

Fig. 2 Microstructure in the thickness direction of the lab-processed sheet with thickness of 1.6 mm, annealed at 400 °C for 90 min and aged at 160 °C for 15 h (**a**) Microstructure in the center region, (d_l = 20 μm, d_t = 2.0 μm), (**b**) microstructure in the near-surface region (d_l = 18 μm, d_t = 1.5 μm)

continuous casting. The coarse second-phase particles have been identified as Al–Fe–Mn phase in the same continuous cast 5052 alloy in previous research [1]. Furthermore, it can be found that there are more coarse particles in the center region than in the near-surface region of the specimens. The difference in number of particles is caused by centerline segregation formed during continuous casting as a result of intensive segregation of alloying elements in the plate center plane [2]. It can also be found that there are more coarse particles in the 0.8 mm thick lab-processed sheet than in the 1.6 mm thick lab-processed sheet, indicating that the centerline segregation of the second-phase particles is aggravated with increasing the rolling reduction. It is believed that this difference is due to the movement of the particles toward the centerline plane with the flow of matrix during plastic deformation in cold-rolling. This is consistent with previous finding that a banded constituent particle structure along the rolling direction is found in the continuous cast 5052 alloy sheet after 90% cold-rolling [1]. The centerline segregation may influence the mechanical property and formability of the lab-processed sheets with different thickness, which will be discussed in Sect. Microstructure of the lab-processed sheet and Sect. Mechanical Behavior, in detail.

Another noticeable difference between the microstructures in the center region and in the near-surface region of the specimens is grain size. The grains in the near-surface region are finer than those in the center region. For example, for the 0.8 mm thick lab-processed sheet, the average length (d_l) and average thickness (d_t) of the elongated grains in the near-surface region are 10 and 1.3 μm, respectively, whereas the corresponding values in the center region are 13 and 1.8 μm, respectively. Moreover, the grains in the sheet of 0.8 mm are somewhat finer than those in the sheet of 1.6 mm by comparing the average length and average thickness of the grains in the same locations of the two specimens. This is also consistent with previous finding that the grain size decreases with increasing cold-rolling reduction [1].

Mechanical behavior

Figure 3 shows plots of engineering stress versus engineering strain for the lab-processed sheets and the in-line annealed sheets annealed at different temperatures. The mechanical properties for all the investigated sheets and 5052-O sheet produced by conventional method are summarized in Tables 1 and 2 [12, 13]. All the curves of engineering stress versus strain exhibit serrated flow, which is a reflection of dynamic strengthening of Portevin–Le Chatelier effect [11]. The lab-processed sheet annealed at 400 °C for 90 min has the best ductility, as indicated by the largest engineering strain at fracture (Fig. 3a) and elongation (Table 1). For determination of the forming limit

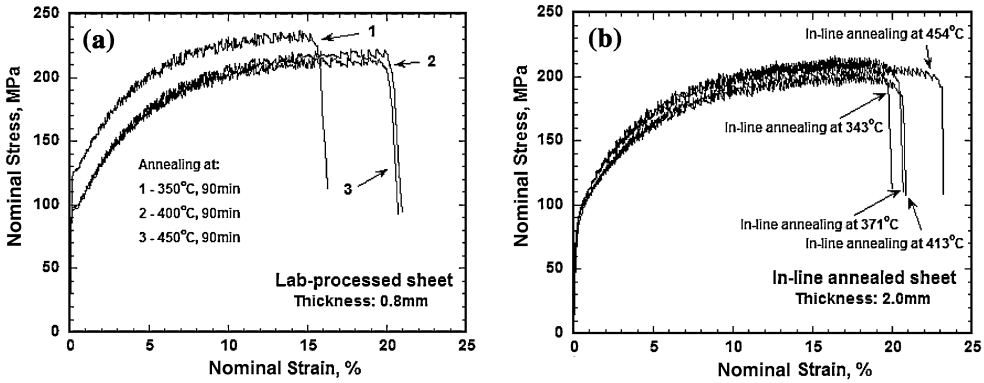

Fig. 3 Nominal stress–nominal strain curves for continuous cast 5052 alloy sheets. (**a**) Lab-processed sheet, (**b**) in-line annealed sheet

Table 1 Mechanical properties of the lab-processed sheets and conventionally produced 5052-O Al sheet

Material	YS (MPa)	UTS (MPa)	El (%)	n_1	K_1 (MPa)	n_2	K_2 (MPa)
Conventional 5052-O sheet	90	193	25	0.28			
Lab-processed sheet (1.6 mm)	102.1	215.1	21.1	0.312	455	0.2	358
Lab-processed sheet (0.8 mm)	97.9	217.3	20	0.338	517.9	0.192	362

curve, all the lab-processed sheet specimens were subjected to the annealing at 400 °C for 90 min. Compared with the lab-processed sheets, the in-line annealed sheets do not have evident yield points (Fig. 3b). The sheet annealed at 454 °C exhibits larger engineering strain at fracture (or elongation in Table 2) than other sheets (Fig. 3b).

The logarithmic curves of true stress versus true strain for the lab-processed sheets and the in-line annealed sheets have been plotted, and the lab-processed sheet annealed at 400 °C for 90 min and the in-line annealed sheet annealed at 454 °C are typically shown in Fig. 4. From the slope of the best linear fit through the plot of true stress and strain, the values of strain-hardening exponent n and strength coefficient K can be determined. It is found that all of these sheets exhibit two-stage strain hardening behavior i.e. the terminal values of the strain-hardening exponent, n_2, are substantially less than the earlier constant values, n_1, in all plots. As shown in Fig. 4a, a constant value of n ($n_1 = 0.338$) for the lab-processed sheet can be determined from early part of the curve, whereas a smaller n ($n_2 = 0.192$) can be obtained on the basis of the last portion of the stress–strain data prior to maximum load. The strength coefficient K_1 and K_2 corresponding to n_1 and n_2 are 517.9 and 362.0 MPa, respectively. For the in-line annealed sheet annealed at 454 °C (Fig. 4b), n_1 and K_1 are 0.300 and 417.2 MPa, respectively, n_2 and K_2 are 0.228 and 359.2 MPa, respectively. Furthermore, it can be found that the n_2-values are much closer to the uniform strains than the n_1-values. For example, the uniform strain for the 0.8 mm thick lab-processed sheet is about 0.192 (Fig. 3a), equal to the n_2-value of 0.192, while much smaller than the n_1-value of 0.338. Clearly this terminal n value, designated as n_2, is related to maximum load condition and becomes equal to uniform strain, and thus marks the onset of diffuse necking [14]. One possible mechanism for this drop in n immediately prior to the maximum load is the ease of cross slip leading to an exhaustion of strain hardening [15]. From Tables 1 and 2, it can also be found that the n_2-values are closer to the values of the total elongation. These results indicate that the specimen failed at the strain slightly higher than that at the onset of diffuse neck, i.e. almost all the total elongation comes from the uniform strain. In addition, the in-line annealed sheet annealed at 454 °C exhibits the largest value of n_2, indicating that this sheet experienced more uniform deformation during tensile tests.

From Table 1, the sheets obtained from continuous cast product appear to have somewhat higher strength and slightly lower elongation compared with the con-

Table 2 Mechanical properties of the in-line annealed sheets with thickness of 2.0 mm

In-line annealing temperature	YS (MPa)	UTS (MPa)	El (%)	n_1	K_1 (MPa)	n_2	K_2 (MPa)
343 °C	94.4	249.8	20	0.312	454.4	0.191	344.4
371 °C	95.8	251.1	20.7	0.303	444.8	0.204	351.8
413 °C	88.9	238.3	20.9	0.296	417.2	0.21	337.1
454 °C	90.3	250	23.2	0.3	417.2	0.228	359.2

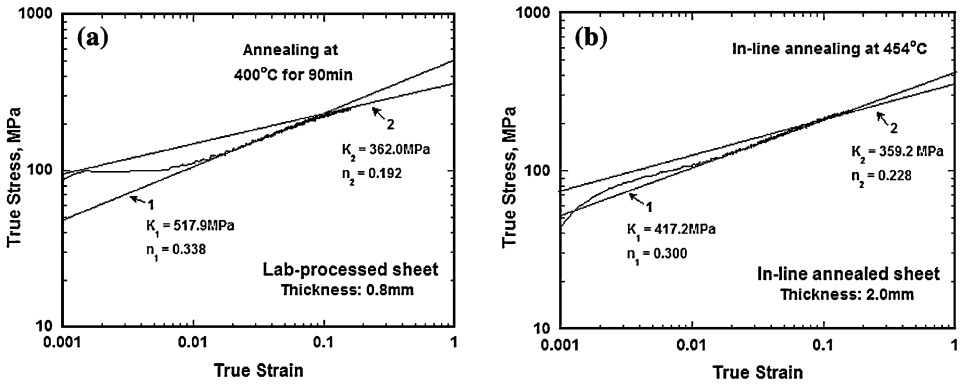

Fig. 4 True stress–true strain curves for continuous cast 5052 alloy sheets. (**a**) Lab-processed sheet annealed at 400 °C for 90 min, (**b**) in-line annealed sheet annealed at 454 °C

ventional 5052-O Al sheet. It can also be found that the 0.8 mm thick lab-processed sheet has higher ultimate tensile strength (UTS) and strength coefficient K, and lower tensile elongation and n_2-value than the 1.6 mm thick lab-processed sheet, which means that the strength increases and the ductility decreases with increasing rolling reduction. This may be related to the presence of segregation along the centerline of the continuous cast plate. The second-phase particles segregated along the centerline plane may cause strengthening [8]. The strengthening in thin sheet rolled from the continuous cast plate is increased to a greater extent than that in the thick sheet. On the other hand, the centerline segregation of the second-phase particles is aggravated with increasing rolling reduction in the lab-processed sheets. Therefore, the contribution of second-phase particles to sheet strengthening increases with increasing rolling reduction. However, the second-phase particles can initiate voids, and thus results in earlier fracture, leading to a lower ductility. This is demonstrated by the smaller post-uniform strain in the 0.8 mm lab-processed sheet, as indicated by the fact that the n_2-value is much closer to the total elongation (Table 1). Also, the grain refinement by cold-rolling and annealing may give a contribution to the increase of the strength. In addition, it is speculated that the difference in mechanical properties between the conventionally produced 5052-O sheet and the continuous cast 5052 sheet is also due to the centerline segregation of the second-phase particles.

From Table 2, it is evident that with increasing the annealing temperature for the in-line annealed sheets, the elongation and n_2-value increase, whereas the strength properties exhibit less change. As a result, the sample annealed at 454 °C exhibits a good combination of strength and ductility. These results indicate that the in-line annealing temperature of 454 °C is the optimum annealing condition for good mechanical properties. Compared with the lab-processed sheets, the in-line annealed sheet annealed at 454 °C exhibits higher UTS and elongation, and lower yield strength.

Determination of forming limit curves

During punch stretch testing, cracks initiate at the region where the strain is largest, and propagate to fracture. Grid circles near the middle of crack reach to the highest strain and are used to construct a forming limit curve as failed circles. The necking circles are selected on opposite side of the crack in the deformed specimens where incipient necking is observed. Figure 5 shows how to obtain a datum from the plot of measured strains for constructing the FLC. In the plot, the data from circles cut through by a crack are labeled to be ''fracture'', and those from circles near necking are labeled to be ''neck'', and others are ''success''. The datum of the limit strain is obtained from the

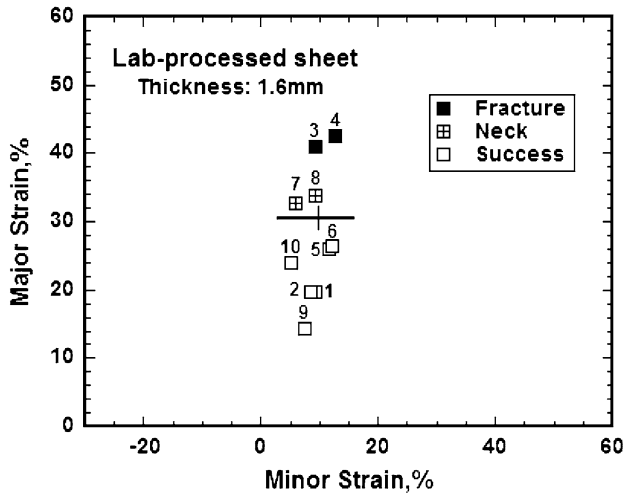

Fig. 5 A plot of measured strains for the lab-processed sheet with thickness of 1.6 mm

middle of the acceptable data points (marked as ''success'') and the necked or fractured data points. Furthermore, the FLC is drawn through fitting the four data obtained from four tests by varying the lubrication or reducing the specimen width as described in Sect. Experimental procedure.

Figure 6 shows forming limit curves of the lab-processed sheets, and sheets fabricated by conventional method [16]. It is clear that the 1.6 mm thick lab-processed sheets have higher limit strains than the 0.8 mm thick lab-processed sheets. Thick sheets appear to spread the neck over a larger region and fail at higher limit strains. Moreover, material on the outside of sheet during bending in punch stretch tests suffers larger strains than that on the centerline of the sheet, and thus, thicker layer of finer grains in the near-surface region may also give a contribution to higher limit strains of the 1.6 mm thick sheet specimens. On the other hand, as in the uniaxial tensile tests, the voids may initiate earlier during punch stretch testing due to the presence of the second-phase particles toward the center of the sheets [17]. The increasing contribution of the second-phase particles on fracture in the thinner sheet might also lead to lower limit strains of the lab-processed thin sheet. From Fig. 6, the forming limit curve of the 0.8 mm thick lab-processed sheet is lower than that of conventionally produced 5052-O Al, and close to that of 6111-T4 Al sheet, which is a standard material in the automotive industry. However, the 0.8 mm thick lab-processed sheet has greater formability under biaxial tension than the 6111-T4 Al sheet. Therefore, it is expected that the sheet could be used in automotive industry to minimize part cost.

Figure 7 shows forming limit curves of the in-line annealed sheets. It can be found that when the minor strains are less than 0, the limit strains increase with increasing the annealing temperature. This may be related to the higher n_2-values, i.e. larger uniform strains in uniaxial tensile tests, at higher annealing temperatures (Table 2). However, the annealing temperature has not significantly effect on the limit strains under biaxial tension. In addition, compared with the forming limit curves of the lab-processed sheets in Fig. 6, all the in-line annealed sheets have higher limit strains. For example, the minor strain corresponding to plane strain for the in-line annealed sheet annealed at 454 °C is about 33, which is higher than that of 28 for the 1.6 mm thick lab-processed sheets. These results demonstrate that the in-line annealing heat treatment results in the production of continuous cast alloy sheet with improved formability.

Conclusions

(1) The lab-processed sheets exhibit somewhat inhomogeneous microstructures due to centerline segregation of the second-phase particles. The cold-rolling process aggravates the centerline segregation, and refines the grain size with annealing.

(2) All the lab-processed sheets show evident yield behavior. The annealing heat treatment at 400 °C for 90 min produces the best ductility in the lab-processed sheet. Increasing rolling reduction results in an increase of UTS and a decrease of ductility due to increasing contribution of centerline segregation of the second-phase particles. For the in-line annealed sheets, increasing the

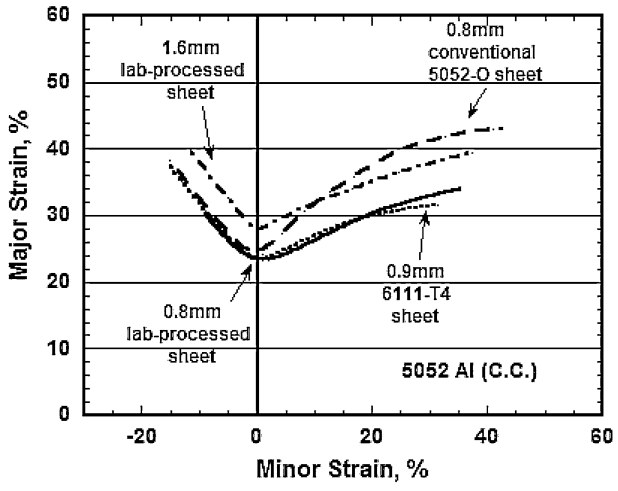

Fig. 6 Forming limit curves for the lab-processed sheets and conventionally produced aluminum sheets

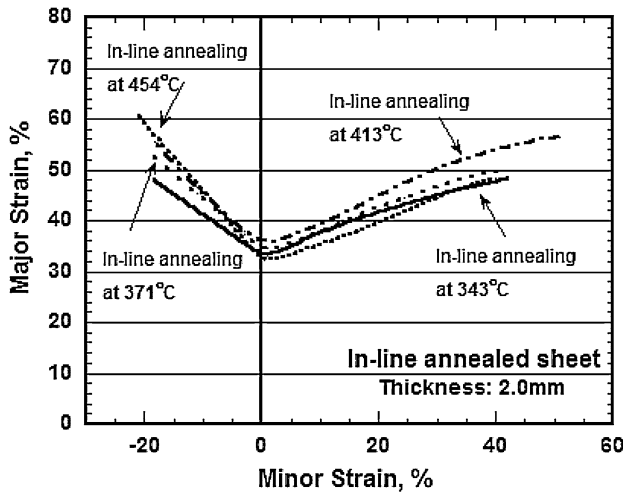

Fig. 7 Forming limit curves for the in-line annealed sheets

annealing temperature leads to an increase of elongation and less change of strength properties. The in-line annealed sheet annealed at 454 °C exhibits a good combination of strength and ductility.

(3) Both the lab-processed sheets and the in-line annealed sheets exhibit two-stage strain hardening behavior. The values of n_2 are equal to the uniform strains, and thus mark the onset of diffuse necking. Increasing rolling reduction decreases the n_2-value for the lab-processed sheets, and the in-line annealing temperature of 454 °C produces the largest n_2-value.

(4) The 1.6 mm thick lab-processed sheets have higher limit strains than the 0.8 mm thick lab-processed sheets. The increasing contribution of the second-phase particles on fracture in the thinner sheet might give a contribution to the lower limit strains. The level of the forming limit curve of the 0.8 mm thick lab-processed sheet is lower than that of conventionally produced 5052-O Al, and close to that of 6111-T4 Al sheet, but excellent formability is recorded under biaxial tension. It is expected that the continuous cast alloy sheets could be used in automotive industry.

(5) For the in-line annealed sheets, the levels of the forming limit curves in the negative values of the minor strain increase with increasing the annealing temperature. This is consistent with the increase of the n_2-value. However, the annealing temperature has not significant effect on the levels of the forming limit curves under biaxial tension. Compared with the lab-processed sheets, the in-line annealed sheet annealed at 454 °C has higher level of the forming limit curve besides its higher values of UTS, elongation and n_2. Therefore, the in-line annealing process results in the production of continuous cast alloy sheet with improved formability.

References

1. Liu J, Morries JG (2004) Mater Sci Eng A385:342
2. Slámová M, Karlík M, Robaut F, Robaut F, Sláma P, Véron M (2002) Mater Characterization 49(3):231
3. Haga T, Nishiyama T, Suzuki S (2003) J Mater Process Technol 133(1–2):103
4. Zhou SX, Zhong J, Mao D, Funke P (2003) J Mater Process Technol 134(3):363
5. Hecker SS (1975) Sheet Met Ind 52:671
6. Ghosh AK (1978) In: Koistinen DP and Wang NM (eds) Mechanica of sheet metal forming. Plenum Press, New York, pp 287–312
7. Moshksar MM, Mansorzadeh S (2003) J Mater Process Technol 141(1):138
8. Hosford WF, Caddell RM (1993) Metal forming: mechanics and metallurgy, 2nd edn. PTR Prentice Hall, Englewood Cliffs, NJ
9. Yao H, Cao J (2002) Int J Plasticity 18(8):1013
10. Stoughton TB (2000) Int J Mech Sci 42:1
11. Samuel M (2004) J Mater Process Technol 153–154(10):424
12. Aluminum Standards and data (1993) The Aluminum Association, Inc
13. Hecker SS (1974) Mater Eng Q 11:30
14. Ghosh AK (1977) J Eng Mater Technol 7:264
15. Honeycomb RWK (1968) The plastic deformation of metals. Edward Arnold Publishers, pp 228
16. Hecker SS (1975) J Eng Mater Technol 1:66
17. Ragab AR, Saleh ChAR (2000) Mech Mater 32:71